ELECTRON RING ACCELERATOR

Uwe Schumacher

Max-Planck-Institut für Plasmaphysik
Association EURATOM - IPP, D-8046 Garching

I. Introduction

The electron ring accelerator (ERA) is one example of collective ion accelerators that make use of non-vanishing currents (curl $\vec{B} = 0$) and charges (div $\vec{E} = 0$) at the location of the accelerated particle. Its origin dates back to the CERN Symposium on High-Energy Accelerators and Pion Physics in 1956 with V.I. Veksler's /5/ suggestions of acceleration methods by means of collective fields and G.I. Budker's /6/ proposed concept of a self-stabilized ring beam. The idea of electron ring acceleration by using the internal electric field of an intense ring of electrons gyrating in a magnetic field received widespread attention after the announcement of the experimental program on ERA at Dubna by V.I. Veksler, V.P. Sarantsev and their coworkers /7/ at the Cambridge High Energy Accelerator Conference in 1967, after which electron ring accelerator work was initiated in many different countries. The electron ring accelerator was regarded as an efficient ion acceleration method, and the question arose, if it might open a cheap path to very high energy protons /7,8,9/. The following report on the ERA work will give an answer to this question.

II. Principles

In the electron ring accelerator the collective fields are generated by the charges of a ring of relativistic electrons in which the ions to be accelerated are embedded. Usually the ring is formed by injecting an intense relativistic electron beam into a magnetic field. The electrostatic repulsion of the charges is compensated by the magnetic attraction in the high ring current and the ion loading of the ring /6,7/. There are four different schemes of electron ring accelerator devices, schematically drawn in Fig. 1, two of them applying ring compression prior to ring acceleration. In the transverse ERA concept (upper left), proposed by the Lecce-Bari-group /10/, an intense electron beam is injected into an inhomogeneous magnetic field (with gradient $\nabla\vec{B}$), perpendicular to the field lines. The $\nabla\vec{B}$-drift moves the ring-shaped structure perpendicular to $\vec{B}$ and to $\nabla\vec{B}$. If the magnetic field gradient increases in space hence the rings and the embedded ions are accelerated. Preliminary experiments on this basis and an extension to toroidal geometry were performed at Lecce.

In the cusp field ERA (upper right in Fig. 1) /11,12/ the electron rings are formed from hollow electron beams (injected from the left side in Fig. 1) in a static magnetic field. Due to the constancy of the canonical angular momentum the initially longitudinally (i.e. parallel to the magnetic field axis) directed electron velocity can be transformed into azimuthally oriented velocity after the transition through the cusped magnetic field structure. This scheme was applied in the University of Maryland experiments /12/ to accumulate electrons into intense rings, that after ion loading can be accelerated parallel to the magnetic field axis.

In order to increase the electron density and hence the electric field strength in the ring that holds the ions during

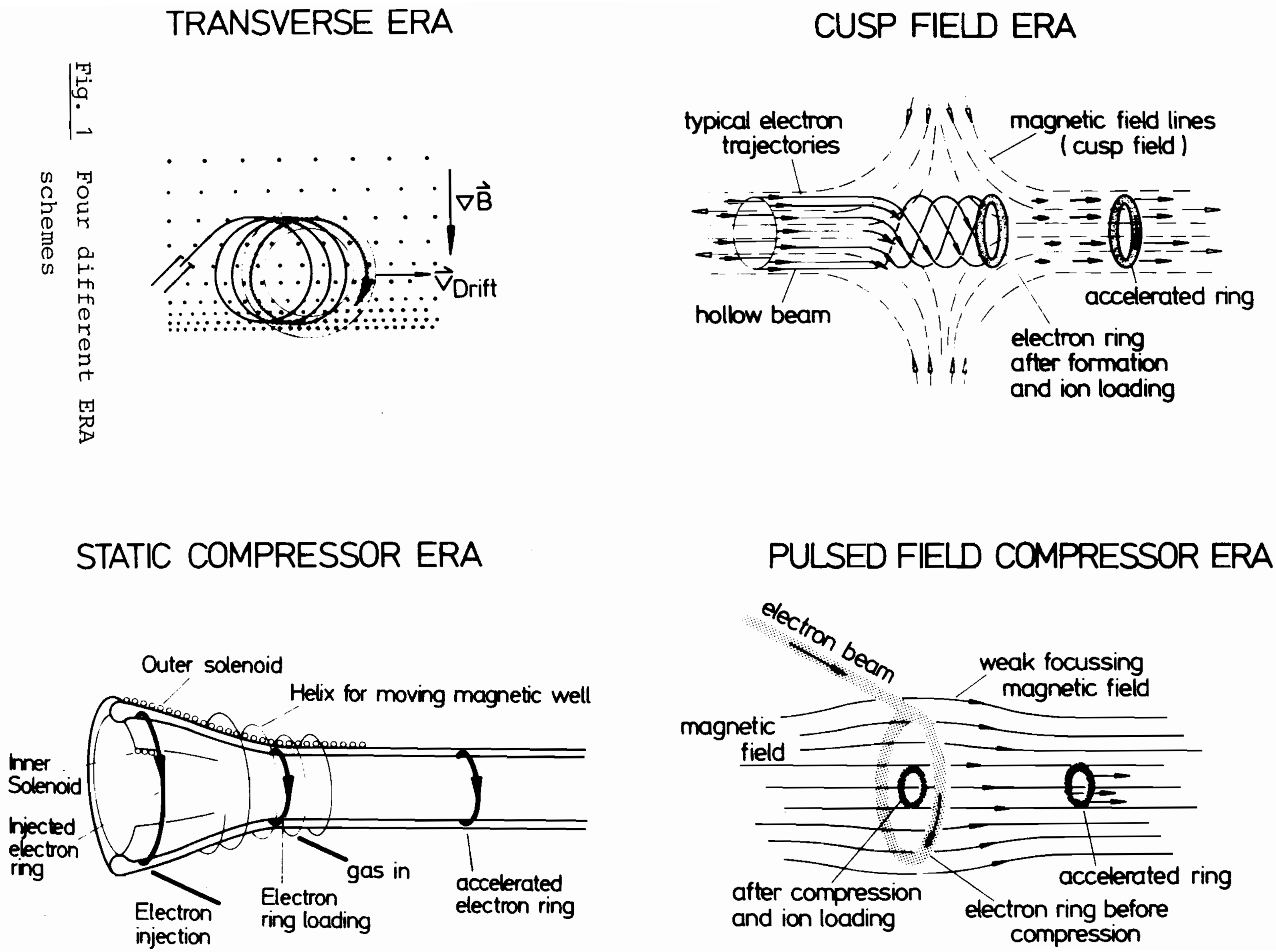

Fig. 1 Four different ERA schemes

the ring acceleration, ring compression is applied. One method (lower left in Fig. 1), proposed by Christophilos /13/ and by Laslett and Sessler /14/, performs compression in the static magnetic field by a suitable choice of its shape, such that energy and canonical angular momentum are conserved, before ion loading and acceleration can start. This scheme has not yet been experimentally tested.

In the pulsed field compressor ERA device (lower right in Fig. 1), the most intensively investigated scheme, an unneutralized electron beam is injected into a slightly focussing magnetic field to provide axial focussing of the formed ring as long as ions are missing. The major and minor ring dimensions in this device are compressed (and thus the electric field strength is increased) by increasing the magnetic field amplitude as a function of time. To compensate the difference between electrostatic repulsion and magnetic attraction, which is of the order of $1/\gamma^2$ of the electrostatic force the ring is partly neutralized by ions of charge Z and number N_i, which are created by collisional ionization of the residual gas just in the potential well of the electron ring (of electron number N_e). Hence in a homogeneous magnetic field the ring is in equilibrium, if the Budker-limits /6/

$$\text{(1)} \qquad \frac{1}{\gamma^2} < \frac{Z\, N_i}{N_e} < 1$$

are fulfilled.

The maximum electric field strength of a slender ring of major radius R and minor radius a containing N_e electrons is /1-4/

$$(2) \quad E_{max} = -\frac{e}{4\pi^2 \varepsilon_o R} \cdot \frac{N_e}{a} = \frac{4.58 \cdot 10^{-12} N_e}{R\,[\mathrm{cm}] \cdot a\,[\mathrm{cm}]} \left[\frac{\mathrm{MV}}{\mathrm{m}}\right] =$$

$$= 6 \cdot \frac{I_e\,[\mathrm{kA}]}{\beta \cdot a\,[\mathrm{cm}]} \left[\frac{\mathrm{MV}}{\mathrm{m}}\right]$$

with the electron current

$$I_e = \frac{N_e e \beta c}{2\pi R}$$

and the electron velocity βc (c = speed of light).
The holding power E_H of the ring, i.e. the maximum field strength in the accelerated ring, however, is smaller by a factor of η:

$$(3) \quad E_H = \eta\, E_{max} \quad \text{with } 0.2 < \eta < 0.8,$$

due to the polarization of the ring during the acceleration. This may be seen from Fig. 2, where according to simulation calculations by Hofmann /15/ the density distributions of ions and electrons in a ring cross section are plotted for 4 different acceleration field strengths. It is obvious that for high acceleration field strength the ring is strongly polarized in axial direction thus lowering the ring holding power.
There are, however, methods to increase the holding power E_H (up to about $\eta \simeq 0.8$) by enhancing the axial focussing, e.g. with "squirrel cage"-structures (Fig. 3) for image focussing. These stripe-like structures generate nearby electric (but far magnetic) images of the electron ring, so that due to this additional axial focussing even unloaded electron rings can

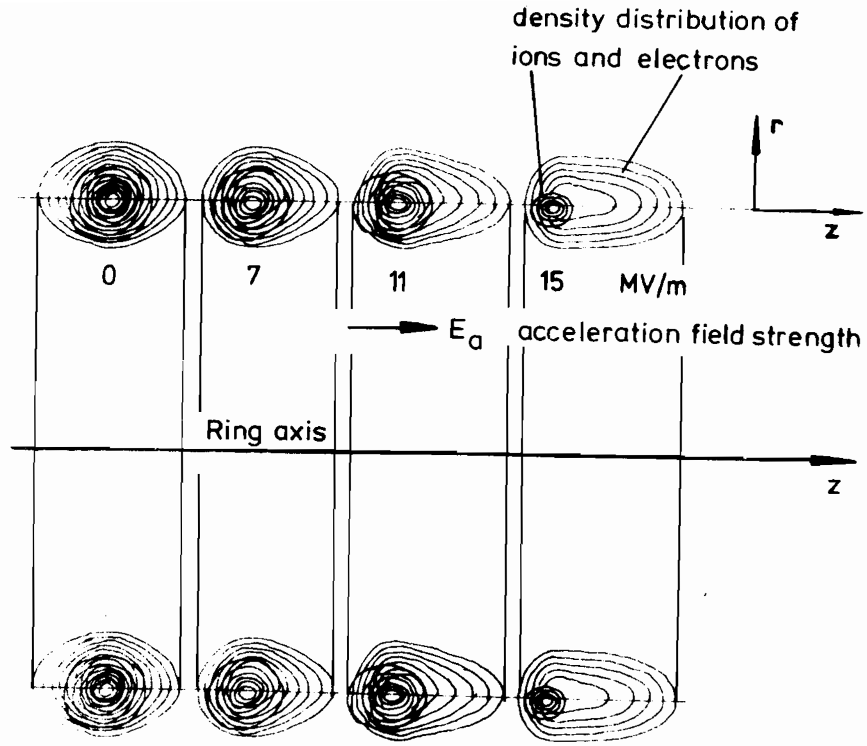

Fig. 2 Reduction of the ring holding power E_H during acceleration due to ring polarization (after simulation calculations by Hofmann /15/)

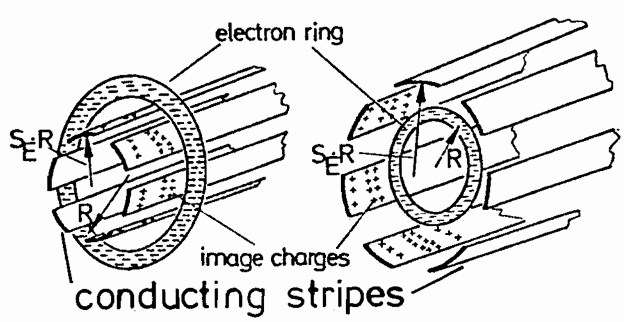

Fig. 3 Electron ring image focussing by "squirrel cage" structures

be stable and hence can be accelerated, as was experimentally verified. The left Budker limit in the inequality (1) thus can be extended to zero.

The image fields from the squirrel cage give focussing for the axial direction and defocussing for the radial direction, which is seen from the expressions (and their specific meanings) for the radial (ν_r) and axial (ν_z) betatron tunes /3,16/

$$\nu_r^2 = \underbrace{(1 - n)}_{\text{external field focussing}} + \mu\Bigg\{\frac{2R^2}{\sigma_a(\sigma_a + \sigma_b)}\Big(\underbrace{f}_{\text{ion focussing}} - \underbrace{\frac{1}{\gamma^2}}_{\text{electron defocussing}}\Big) + \underbrace{(1 - f)\frac{P}{2}}_{\text{toroidal effect (focussing)}} \tag{4a}$$

$$- \underbrace{4\left[\frac{(1 - f)\epsilon_{1,E}}{(S_E - 1)^2} - \frac{\epsilon_{1,M}}{(S_M - 1)^2}\right]}_{\text{image field (defocussing)}} - \underbrace{n\left[(1 - \frac{f}{2})P + (1 - f)K - \bar{L}\right]}_{\text{applied-field correction due to self-fields}}\Bigg\}$$

$$\nu_z^2 = \underbrace{n}_{\text{external field focussing}} + \mu\Bigg\{\frac{2R^2}{\sigma_a(\sigma_a + \sigma_b)}\Big(\underbrace{f}_{\text{ion focussing}} - \underbrace{\frac{1}{\gamma^2}}_{\text{electron defocussing}}\Big) - \underbrace{(1 - f)\frac{P}{2}}_{\text{toroidal effect (defocussing)}} \tag{4b}$$

$$+ \underbrace{4\left[\frac{(1 - f)\epsilon_{1,E}}{(S_E - 1)^2} - \frac{\epsilon_{1,M}}{(S_M - 1)^2}\right]}_{\text{image field focussing}} + \underbrace{n\left[(1 - \frac{f}{2})P + (1 - f)K - \bar{L}\right]}_{\text{applied-field correction due to self-fields}}\Bigg\}$$

with

$$\mu = \frac{N_e r_o}{\gamma 2\pi R} = \frac{\nu_{Budker}}{\gamma} \qquad f = Z_i N_i / N_e$$

$$P = 2 \ln\left[\frac{8\sqrt{2}R}{\sigma_a + \sigma_b}\right] \qquad K \simeq 1/(S_E - 1)$$

$$\bar{L} \simeq 1/(S_M - 1) \quad .$$

III. Electron Ring Acceleration

3.1 Acceleration by electric fields

The energy gain of ions in the electron ring by acceleration in an electric field strength ε is given by

$$dE_i/dz = e\varepsilon\frac{M_i}{\gamma_c m_e}\left[\frac{1 - ZN_i/N_e}{1 + N_i M_i/N_e m_e \gamma_c}\right](1 - \alpha_c N_e) \tag{5}$$

where $\gamma_c m_e$ is the electron mass. This energy gain is not only reduced by the ion to electron mass ratio (the ring inertia due to ion loading) and the ion charge ZN_i in the ring, but also by the energy loss due to cavity radiation, which occurs when the intense ring charge passes by the cavities for electric field (rf) acceleration, expressed by the last bracket. According to numerical calculations by Keil /17/ the parameter α_c is a very sensitive function of the cavity radius. The reduction in energy gain is already as large as by a factor of 2 for an electron number of $N_e = 3 \cdot 10^{13}$, an electric field strength $\varepsilon = 5$ MV/m and a cavity radius of 10 cm. Hence for acceleration by electric fields the field strength has to be limited by

$$\varepsilon \lesssim E_H Z \frac{m_e \gamma_c}{M_i} \frac{1 + N_i M_i / N_e m_e \gamma_c}{(1 - ZN_i/N_e)(1 - \alpha_c N_e)} \qquad (6)$$

where the holding power E_H has to be taken with $\eta \simeq 0.2$ (according to equ. (3)), because squirrel cage focussing cannot be applied in combination with electric field (cavity) acceleration.

These limiting effects exclude the electron ring accelerator as a candidate for very high energy proton accelerators.

The deleterious property of strong cavity radiation excited by the electron ring as a compact charge bunch, however, might be an advantage for other acceleration mechanisms, e.g. the wake field accelerator (see T. Weiland).

3.2 Magnetic expansion acceleration

The magnetic expansion acceleration makes use of the Lorentz force of the azimuthally (at a speed of β c) rotating electrons in the radial magnetic field component B_r as axial driving force (see Fig. 4), so that the energy gain of the ions in the electron ring is given by

$$dE_i/dz = e\beta_{\perp}cB_r \frac{M_i}{\gamma m_e} \frac{1}{1 + N_iM_i/N_em_e\gamma_c} \quad . \tag{7}$$

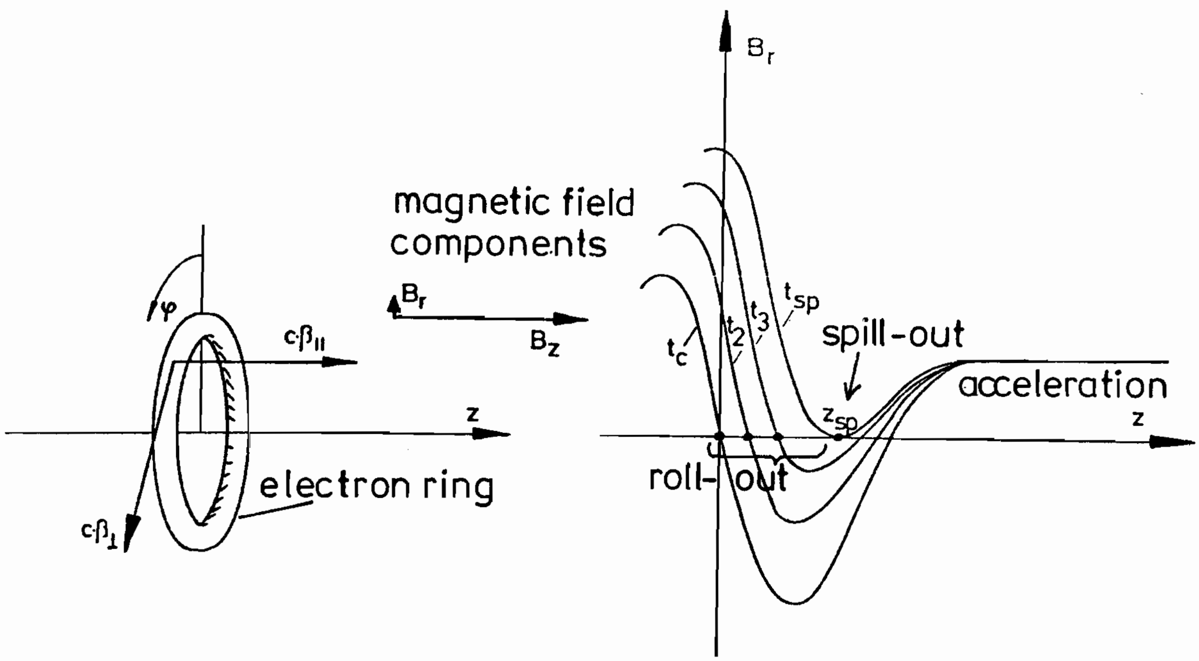

Fig. 4 Ring geometry and magnetic field components (left) and axial distribution of the radial magnetic field component from roll-out through spill-out to ring acceleration (right).

In order not to loose the ions from the electron ring during magnetic expansion acceleration the radial magnetic field component must be limited by

$$B_r \leq E_H Z \frac{m_e\gamma_c}{c\beta_{\perp}M_i}(1 + N_iM_i/N_em_e\gamma_c) \tag{8}$$

However, for the magnetic expansion acceleration method the energy given to the ions has to come from the electron kinetic energy, and as a consequence of the conservation of the total energy and the canonical angular momentum the electron ring expands during the acceleration, and the holding power decreases. Hence the attainable ion kinetic energy expressed with its $\gamma_{\parallel}$-value (in axial direction),

$$E_i = (\gamma_{\parallel} - 1)\ M_i\ c^2,$$

is limited, as plotted in Fig. 5 as function of the relative acceleration length z/λ_1 with λ_1 being a constant depending on the electron ring properties /3, 18/; b_1 is the magnetic field drop with B_c the magnetic field strength in compressed state, and $g = N_i M_i/(N_e m_e \gamma_c)$ is the ion to electron mass ratio. Although the upper limit of $\gamma_{\parallel}$ seems to be relatively high, especially for low ion loading, a practical upper limit is given by $\gamma_{\parallel} \simeq 1.6$. Thus very high energy proton acceleration cannot be performed by magnetic expansion acceleration.

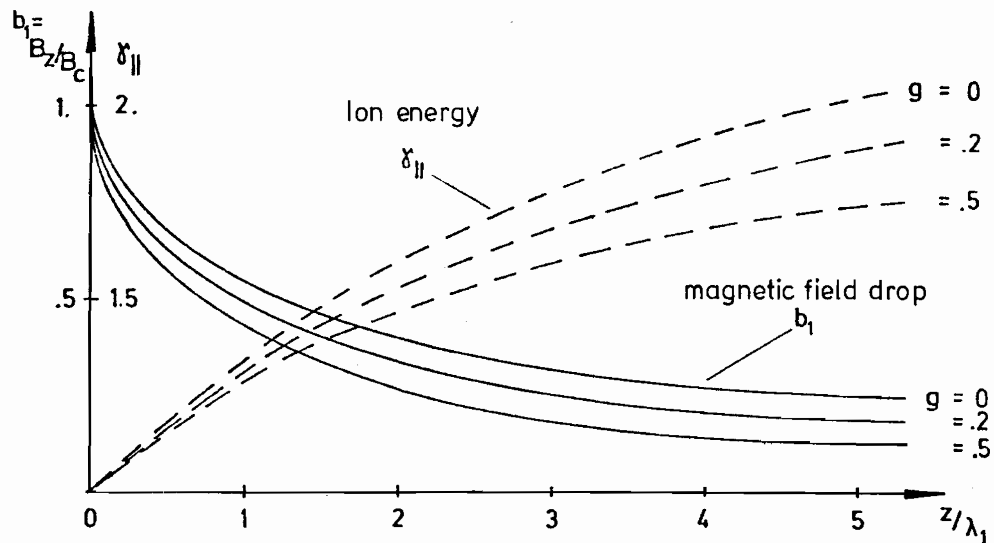

Fig. 5 Magnetic field drop and energy gain versus axial distance for magnetic expansion acceleration

IV. Electron Ring Compression in Pulsed Magnetic Fields

The pulsed field compressor ERA (lower right in Fig. 1) aims at increasing the electron ring holding power by increasing the magnetic field amplitude as a function of time. Due to the conservation of the canonical angular momentum in the axisymmetric field, for nearly homogeneous magnetic field B the flux

$$\phi = \pi R^2 B$$

through the particle orbit is about constant; the magnetic field index $n = -\frac{R}{B} \cdot \frac{\partial B}{\partial R}$ is assumed to be small. This results in the following relations for the major ring radius R, the transverse momentum $p_\perp$, the minor radial half axis a, the minor axial half axis b, and hence with the aid of Equ. (2) for the maximum electric field strength E_{max} after (index 2) and before the compression (index 1)

$$\text{(9)} \qquad \frac{R_2}{R_1} = \left(\frac{B_1}{B_2}\right)^{1/2}, \qquad \frac{p_{\perp 2}}{p_{\perp 1}} = \left(\frac{B_2}{B_1}\right)^{1/2}$$

$$\frac{a_2}{a_1} = \left(\frac{B_1}{B_2}\right)^{1/2} \cdot \left(\frac{1-n_1}{1-n_2}\right)^{1/4}, \qquad \frac{b_2}{b_1} = \left(\frac{B_1}{B_2}\right)^{1/2} \cdot \left(\frac{n_1}{n_2}\right)^{1/4}$$

$$\frac{E_{max2}}{E_{max1}} = \frac{B_2}{B_1} \cdot \frac{1 + b_1/a_1}{\left(\frac{1-n_1}{1-n_2}\right)^{1/4} + \frac{b_1}{a_1}\left(\frac{n_1}{n_2}\right)^{1/4}} .$$

For a nearly homogeneous magnetic field the maximum electric field in the electron ring (and hence the holding power) increases proportionally to the magnetic field strength.

V. Holding Power Reduction and Limitations

5.1 Betatron resonance traversal during compression

The electron ring forming usually occurs at a magnetic field index around n = 0.5, while the acceleration takes place in nearly homogeneous fields with $n \simeq 0$. During the ring compression several betatron (single particle) resonances have therefore to be crossed; these occur when the radial betatron tune ν_r and the axial betatron tune ν_z (see Equ. (4a) and (4b)) are connected by simple integral relations. Laslett and Perkins

/19/ calculated the growth rates of the axial betatron amplitude (in decades per electron revolution) which are plotted in Fig. 6 as a function of the magnetic field index n, median-plane symmetry of the magnetic field is assumed.

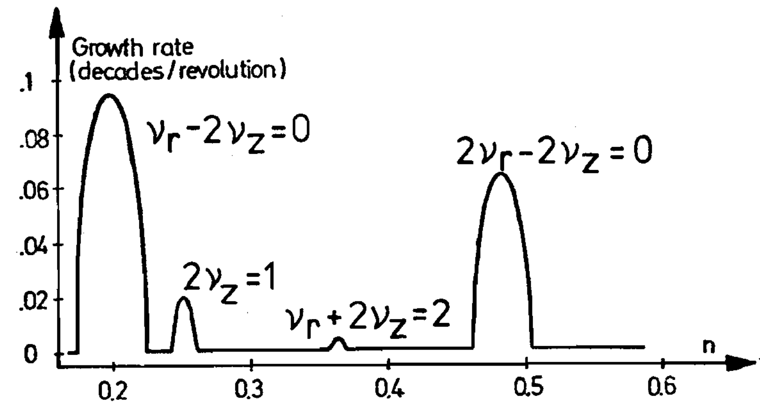

Fig. 6
Axial betatron amplitude growth rates versus magnetic field index n (after Laslett and Perkins /19/)

It turns out that the resonance $\nu_r - 2\nu_z = 0$ around the magnetic field index n = 0.2 (the Walkinshaw resonance) is regarded as potentially dangerous, because it leads to axial beam blow up with high growth rate, as was experimentally observed /20, 21/. Methods of avoiding fast growth during this resonance traversal are a suitable choice of $\partial n/\partial r$ /3, 19/ or very fast resonance traversal /22/, e.g. by very fast ring compression /23/. This procedure, however, is difficult to combine with conducting surfaces near to the ring in order to suppress collective instabilities, treated in the following.

5.2 Longitudinal collective instabilities

Collective instabilities impose severe limitations on the maximum holding power E_H (see Equ. (2) and (3)). The negative mass instability /24/ leads to azimuthal bunching and subsequent blow up of the electron ring, if insufficient phase mixing (Landau damping) associated with finite electron energy spread $\Delta E/E$ is present. The mechanism is obvious from Fig. 7 (right): An excess charge increases the energy of a downstream particle (1) and decreases that of an upstream particle (2) by repulsion, such that due to $d\omega/dE < 0$ these particles are forced to approach and increase the excess charge.

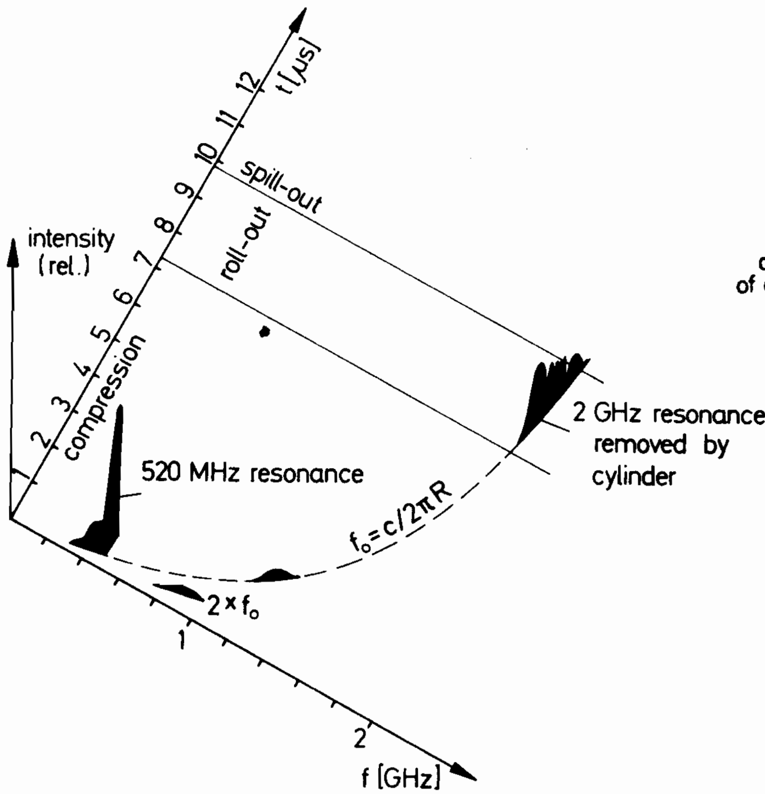

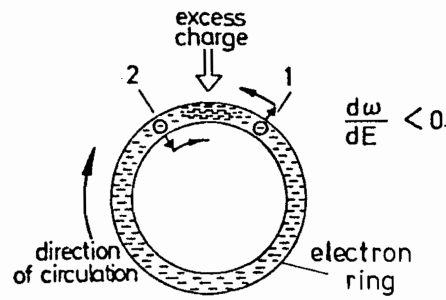

Fig. 7

Negative mass instability mechanism (right) and example of related RF measurements for the Garching fast compression ERA experiment /25/

The associated averaged azimuthal electric field component of the m-th mode $\langle E_{\Theta,m}\rangle$ is related to the current I_m of this mode by

$$\langle E_{\Theta,m}\rangle = \frac{\oint E_{\Theta,m}\,ds}{2\pi R} = -\,Z_m I_m \quad ,$$

where Z_m is the coupling impedance for the m-th mode.

For any energy spread $\Delta E/E$ and a normalized coupling impedance of $|Z_m/mZ_o|$ with $Z_o = (\mu_o/\varepsilon_o)^{1/2} = 377\,\Omega$ the threshold for the electron number N_e in the ring is given by /2, 24/

(10) $$N_e \lesssim \frac{\gamma\, R}{2\beta^3 r_o \left|\frac{Z_m}{mZ_o}\right|} \cdot \left(\frac{\Delta E}{E}\right)^2 \cdot \left[\frac{1}{1-n} - \frac{1}{\gamma^2}\right]$$

and for the holding power E_H using Eqs. (2) and (3)

(11) $$E_H \lesssim \eta \cdot 68.1 \cdot B\,[T] \cdot \frac{\Delta E}{E} \cdot \left(|Z_m| / mZ_o\right)^{-1}$$

with $a/R \simeq 0.7\ \Delta E/E$.

The negative mass instability was extensively investigated by the Berkeley ERA group /26/ and others /27/. Certainly there are relations to other collective instabilities, that are discussed in the following.

5.3 Transverse collective instabilities

The origin of transverse collective instabilities of the electron ring can be associated with nearby resistive walls (resistive wall instability /3, 28/)or with electron-ion collective oscillations /3, 29/. Fig. 8 gives the principle of this transverse collective motion and - in its lower part - oscillograms of the radial magnetic field component of the electron ring

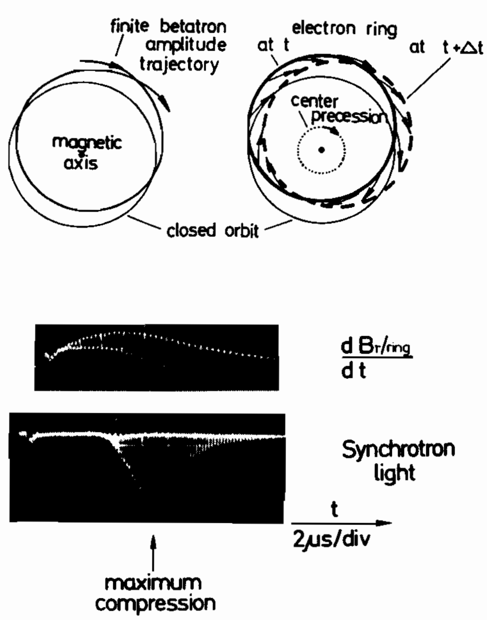

Fig. 8
Principle of transverse collective oscillations at a frequency of $S_c \simeq (1-\nu_r)\,\omega_{ce}$ with $\nu_r \simeq (1-n)^{1/2}$ (top) and their experimental demonstration by magnetic field and synchrotron light measurements /30/

and the synchrotron radiation /30/, by which transverse collective instabilities of very large oscillation amplitude (comparable with the major ring radius) were manifested. The growth rates and collective oscillation frequencies observed in the experiments /23, 26/ were found in very good agreement with theoretical predictions /29/.

VI. Optimum Electron Rings

For optimum electron ring acceleration /31/ the following conditions must be fulfilled:

- Axial focussing must exist, $\nu_z^2 > 0$ (Equ. (4b))
- The negative mass instability threshold (Equ. (10)) must be high
- The Landau damping for transverse instability suppression must be sufficient
- Electron-ion collective instabilities must be avoided.

With B = 2T and $\Delta E/E = 0.1$ one obtains

$$(12) \qquad E_H \; [\mathrm{MV/m}] < \eta \cdot \frac{13.62}{|Z_m / mZ_o|} ,$$

which for an electric acceleration structure with $|Z_m/mZ_o| \simeq 0.5$ and $\eta \simeq 0.2$ (because of lack of image focussing, see Equ. (3)) results in only

$$(13) \qquad E_H \lesssim 5.4 \text{ MV/m} ,$$

while in contrast to this the magnetic expansion acceleration structure with $|Z_m / mZ_o| \simeq 3.2 \;\; \sigma_a/R$ (after Faltens and Laslett /32/), $\Delta E/E \leq 2.36 \cdot \sigma_a/R$ and $\eta \simeq 0.8$ (because of image focussing application) can lead to

$$(14) \qquad E_H \leq 80 \text{ MV/m}.$$

This maximum holding power, however, can be increased linearly with the axial magnetic strength

$$(15) \qquad E_H \; [\mathrm{MV/m}] \lesssim 40.4 \cdot B \; [\mathrm{T}] \, .$$

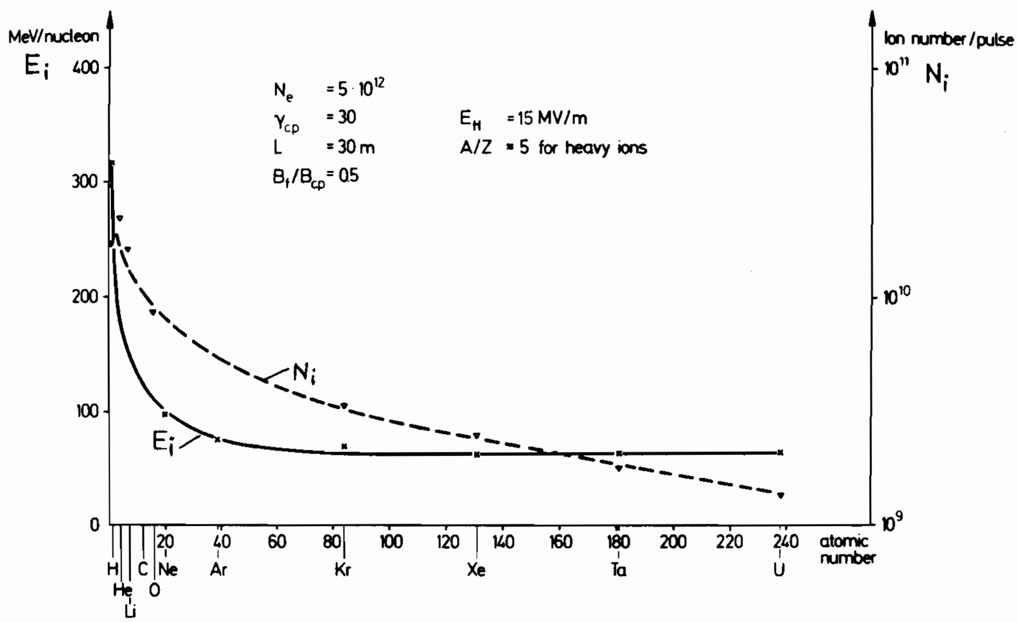

<u>Fig. 9</u> Example of ion energy gain E_i and ion number N_i versus atomic number for a moderate ERA /33/

As an example of the attainable ion energy gain and ion numbers Fig. 9 gives numbers of a moderate quality ERA (15 MV/m holding power), which at a length of only 30 m offers many interesting applications.

VII. Experimental Results

The ERA is an intensively investigated collective acceleration mechanism, that works, although the parameters achieved are far behind the original expectations. The cusp field ERA (upper right in Fig. 1) was carefully studied at the University of Maryland. Intense hollow beams were injected into the cusp magnetic field, and ring formation and stopping could be demonstrated. The rings had small minor dimensions obviously by collective instability suppression at finite electron energy spread.

The pulsed field compressor ERA (lower right in Fig. 1) is being studied at Joint Institute of Nuclear Research (JINR) at Dubna (USSR) since the early sixties, and was investigated at Lawrence Berkeley Laboratory (LBL) at Berkeley (USA), at the MPI für Plasmaphysik at Garching (Germany) and some other laboratories.

At JINR the collective ion acceleration by electron rings was demonstrated by magnetic expansion over a length of about 1 m to an energy of 5 MeV/nucleon, while electric acceleration over a length of about 1.2 m with an electric acceleration field strength of about 6 kV/cm resulted in an energy of 0.8 MeV/nucleon /34/. Recently collective acceleration of Ne, Ar, Kr and Xe ions to 3.2 MeV/nucleon using electric fields instead of the decreasing magnetic field was obtained in the ERA experiments of JINR Dubna. For the near future a 20 MeV/nucleon heavy ion ERA will be constructed as an injector for a high energy heavy ion accelerator.

The LBL investigations on ERA /1,2,26,31,32/ thoroughly helped to clarify many of the important properties of this acceleration mechanism. The experiments mainly dealt with electron ring collective instabilities /26/. Unfortunately the ERA work at LBL was terminated.

The Garching ERA devices aimed at avoiding single particle resonances by very fast ring compression. In a small-scale experiment electron rings of moderate quality (several 10^{12} electrons in a ring of 2.3 cm major radius) allowed a study of the initial phases of collective ion acceleration with the ERA mechanism, the holding power being in the range of 3 to 4 MV/m. Fig. 10 gives schematically the device with the diagnostics /35/ and some oscillograms demonstrating unloaded ring acceleration and ring integrity conservation due to squirrel cage focussing as well as ring inertia increase by hydrogen or helium loading of the electron rings. The upper right part shows the acceleration of hydrogen loaded electron rings versus the ion loading N_i/N_e in agreement with the proportionality to $(1 + N_i M_i/N_e m_e \gamma_c)^{-1}$ in Equ. (7).

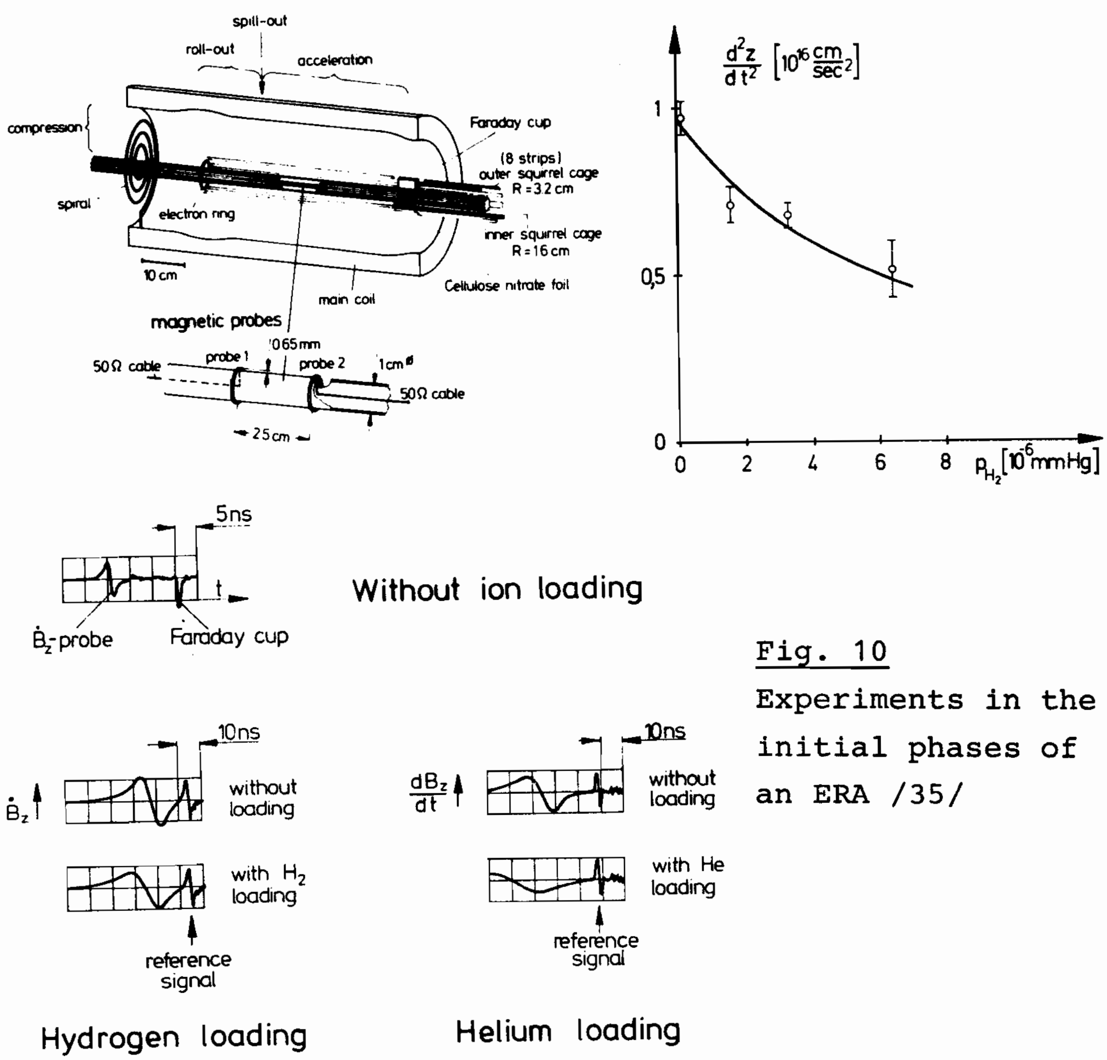

Fig. 10
Experiments in the initial phases of an ERA /35/

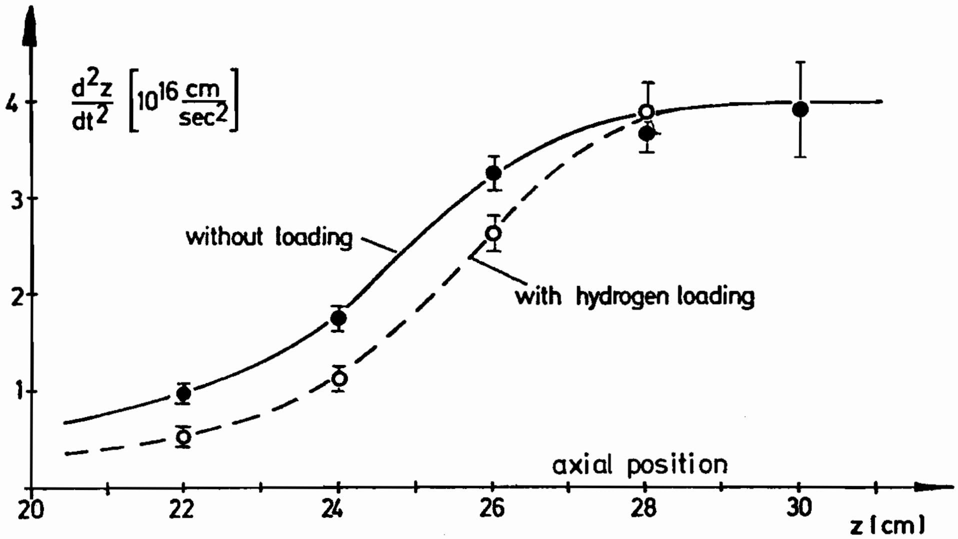

Fig. 11 Measured electron ring acceleration with and without hydrogen loading versus axial distance /35/

From the measurements of the acceleration along the axial distance (Fig. 11) the "holding power" of the electron rings can roughly be determined as the maximum acceleration up to which

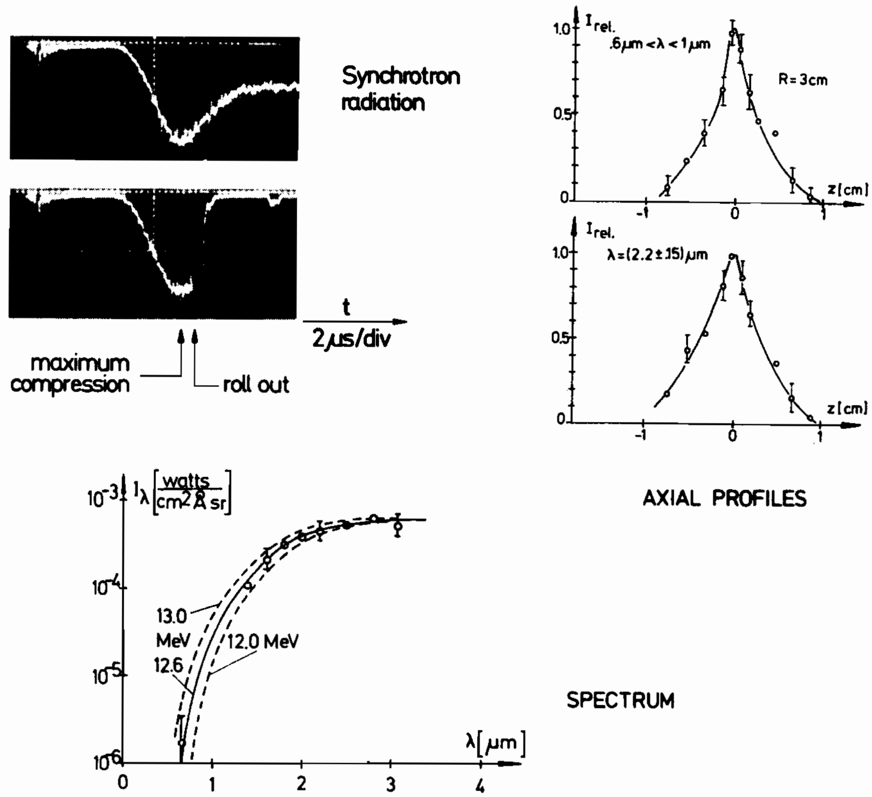

Fig. 12 Electron ring diagnostics by synchrotron radiation measurements /3, 30/

the difference in the ring inertia persists /35/. In the compressed state the rings were investigated by the synchrotron radiation (Fig. 12) /3, 30/.

VII. Conclusions

After nearly 20 years of ERA research /7/ this collective ion acceleration mechanism has been demonstrated to work. The JINR experiments gave heavy ion (noble gas) acceleration to 3.2 MeV per nucleon /34/, the Garching experiments demonstrated the ERA mechanism in the initial phases /35/, and the LBL investigations showed how to master the dangerous collective instabilities /26/. The advantageous application of the ERA seems to be restricted to heavy ion acceleration. For very high energy light ion (proton) acceleration the ERA mechanism seems to be limited to relatively low acceleration field strengths (Equ. (13)), because of lack of image focussing in connection with electric acceleration structures and due to strong energy losses of the ring by cavity radiation (Equ. (5)).

References

General:

/1/ D. Keefe, Particle Accelerators 1, 1 (1970)

/2/ L.J. Laslett, A.M. Sessler, Comments Nuclear Particle Phys. 3, 93 (1969); 4, 211 (1970)

/3/ U. Schumacher, in "Collective Ion Acceleration" by C.L. Olson and U. Schumacher, Springer Tracts in Modern Physics, Vol. 84, Springer-Verlag, Berlin, Heidelberg, New York 1979

/4/ V.P. Sarantsev, E.A. Perelshtein, Collective Ion Acceleration by Electron Rings, Atom Publishers, Moscow 1979

Specific:

/5/ V.I. Veksler, Proc. CERN Symposium on High-Energy Accelerators and Pion Physics, Geneva, Vol. 1, (1956), p. 80

/6/ G.I. Budker, ibid., p. 68, and Atomnaya Energiya 1, 9 (1956)

/7/ V.I. Veksler, V.P. Sarantsev, et al., Proc. 6th Int. Conf. on High-Energy Accelerators, Cambridge, Mass., USA (1967), Cambridge Report CEAL-2000, p. 289 (1967)

/8/ J.D. Lawson, Nature 218, 430 (1968)

/9/ A. Faltens, E. Hartwig, D. Keefe, W. Salsig,IEEE Trans. Nucl. Sci. NS-18, Number 3, 484 (1971)

/10/ I. Boscolo et al., IEEE Trans. Nucl. Sci. NS-20, Number 3, 286 (1973), and Proc. 2nd Int. Conf. on Ion Sources, Vienna (1972), p. 654

/11/ J.G. Kalnins, H. Kim, D.L. Nelson, IEEE Trans. Nucl. Sci. NS-18, 473 (1971)

/12/ M.P. Reiser, IEEE Trans. Nucl. Sci. NS-18, 460 (1971) and IEEE Trans. Nucl. Sci. NS-19, 280 (1972)

/13/ N.C. Christofilos, Phys. Rev. Lett. 22, 830 (1969) and IEEE Trans. Nucl. Sci. NS-16, 1039 (1969)

/14/ L.J. Laslett, A.M. Sessler, IEEE Trans. Nucl. Sci. NS-16, 1034 (1969)

/15/ I. Hofmann, Proc. IXth Int. Conf. on High Energy Accelerators, Stanford (USA), 1974, p. 245

/16/ L.J. Laslett, Proc. 1963 Summer Study on Storage Rings, Accelerators and Experimentation at Super High Energies, Brookhaven National Laboratory,Upton, N.Y., BNL-7534 (1963), p. 324

/17/ E. Keil, Report CERN-ISR-TH/68-49, CERN, Geneva (1968)

/18/ W.B. Lewis, in Proc. Symp. on ERA, LRL Berkeley, USA, Report UCRL-18103 (1968)

/19/ L.J. Laslett, W. Perkins, Nucl. Instr. Meth. 97, 523 (1973)

/20/ D. Keefe et al., Phys. Rev. Lett. 22, 558 (1969)

/21/ C. Andelfinger et al., Report IPP 0/8, MPI für Plasmaphysik, Garching (1971)

/22/ L.S. Barabash et al., Report JINR P9-7697, Dubna (USSR) (1974)

/23/ C. Andelfinger, W. Dommaschk, I. Hofmann, P. Merkel, U. Schumacher, M. Ulrich, Proc. IXth Int. Conf. on High Energy Accelerators, Stanford (USA), p. 218 (1974)

/24/ C.E. Nielsen, A.M. Sessler, K.R. Symon, Int. Conf. on High Energy Accelerators, CERN, Geneva, p. 239 (1959)

/24/ C.E. Nielsen, A.M. Sessler, K.R. Symon, Int. Conf. on High Energy Accelerators, CERN, Geneva, p. 239 (1959); A.A. Kolomenskii, A.N. Lebedev, ibid., p. 115

/25/ U. Schumacher, U. Ulrich, W. Dommaschk, I. Hofmann, P. Merkel, Proc. Int. Topical Conf. on Electron Beam Research and Technology, Albuquerque (USA), p. 385 (1975)

/26/ A. Faltens, G.R. Lambertson, J.M. Peterson, J.B. Rechen, Proc. IXth Int. Conf. on High Energy Acceleration, Stanford (USA), p. 226 (1974)

/27/ P. Merkel, Max-Planck-Institut für Plasmaphysik, Garching, Report IPP 0/39 (1979)

/28/ L.J. Laslett, V.K. Neil, A.M. Sessler, Rev. Sci. Instr. 36, 436 (1965)

/29/ D. Koshkarev, P. Zenkevich, Part. Accel. 3, 1 (1972)

/30/ C. Andelfinger, W. Herrmann, D. Jacobi, A.U. Luccio, W. Ott, U. Schumacher, M. Ulrich, IEEE Trans. Nucl. Sci. NS-20, 276 (1973)

/31/ D. Möhl, L.J. Laslett, A.M. Sessler, Part. Accel. 4, 159 (1973)

/32/ A. Faltens, L.J. Laslett, Part. Accel. 4, 151 (1973)

/33/ C. Andelfinger et al., Max-Planck-Institut für Plasmaphysik, Report IPP 0/30 (1976)

/34/ V.P. Sarantsev, I.N. Ivanov, Proc. 4th Int. Top. Conf. on High-Power Beams, Palaiseau (1981), p. 691

/35/ U. Schumacher, C. Andelfinger, M. Ulrich, Phys. Lett. 51A, 367 (1975) and IEEE Trans. Nucl. Sci. NS-22, 989 (1975)

DISCUSSION

Reiser. A comment about the Maryland experiment. We did stop an electron ring with a resistive wall in a small mirror coil. We also had a concept of ion loading in a fast trapping system, with two small correction coils to kick it out and accelerate it. We were not able to try this out because the work was terminated.

Vaccaro. It is not correct to speak of negative mass instability irrespective of the nature of the coupling impedance. We have negative mass instability only when the coupling impedance above transition is capacitive as it is in a smooth pipe. If the coupling impedance is inductive, (as it generally is if the energy is sufficiently high), we have a resistive wall type instability below transition. If we have an unstable situation the rise time can be much larger in the case of an inductive wall impedance compared to a capacitive wall. This may be interesting for a beam where the rise time is large compared to the operation time.

Schumacher. The subject is complex, and it is difficult to deal with all details in a short presentation, but I agree with your comment.